Parameters that influence charge distribution within metal–quinone complexes include effects of solvation and overall charge in addition to changes in d-orbital energy of the metal resulting from a counterligand effect.

Experimental Section

$Na(diglyme)_2[V(CO)_6]$ was obtained from Strem Chemical Co., and $V(CO)_6$ was prepared by literature procedures.[22] Tetrachloro-1,2-benzoquinone, 3,5-di-*tert*-butyl-1,2-benzoquinone, and 3,5-di-*tert*-butylcatechol were obtained from Aldrich Chemical Co. and recrystallized prior to use. Neutral $V(O_2C_6H_2(t\text{-}Bu)_2)_3$ was prepared by procedures described earlier.[7]

$V(O_2C_6Cl_4)_3$. Tetrachloro-1,2-benzoquinone (2.00 g, 8.2 mmol) in 50 mL of benzene was added dropwise to freshly prepared $V(CO)_6$ (0.55 g, 2.5 mmol) in 50 mL of diethyl ether under Ar. Reaction occurred immediately, giving the dark blue product. The reaction mixture was heated at reflux for 1 h and reduced to half-volume. Dark blue crystals of $V(O_2C_6Cl_4)_3$ separated from solution over a period of several hours as the solution cooled. Analytical data obtained immediately upon isolation of crystals from solution indicated that they form as benzene solvates.

Anal. Calcd for $V(O_2C_6Cl_4)_3\cdot 4C_6H_6$: C, 45.4; H, 2.2; Cl, 38.3; V, 4.7. Found: C, 45.6; H, 2.3; Cl, 38.5; V, 4.6.

$[Na(CH_3OH)_4][V(O_2C_6Cl_4)_3]$. A solution of $[Na(diglyme)_2][V(CO)_6]$ (0.51 g, 1.0 mmol) in 15 mL of CH_3OH was added dropwise to tetrachloro-1,2-benzoquinone (1.23 g, 5.0 mmol) dissolved in 20 mL of toluene. Reaction occurred immediately to give the dark blue microcrystalline product. The volume of the solution was reduced to 20 mL, and the product (0.87 g, 0.87 mmol) was isolated by filtration.

Anal. Calcd for $[Na(CH_3OH)_4][V(O_2C_6Cl_4)_3]$: C, 26.4; H, 1.7; Na, 2.3; Cl, 42.5; V, 5.1. Found: C, 26.3; H, 1.8; Na, 2.2; Cl, 41.8; V, 5.3.

$[Na(CH_3OH)_4][V(O_2C_6H_2(t\text{-}Bu)_2)_3]$. This complex was prepared by the procedure above substituting 3,5-di-*tert*-butyl-1,2-benzoquinone for tetrachlorobenzoquinone.[23]

Anal. Calcd for $[Na(CH_3OH)_4][V(O_2C_6H_2(t\text{-}Bu)_2)_3]$: C, 64.0; H, 8.9; Na, 2.7; V, 5.9. Found: C, 63.2; H, 8.7; Na, 2.8; V, 5.9.

Physical Measurements. Infrared spectra were recorded on a Beckman IR 4250 spectrometer with samples prepared as KBr pellets. UV–vis spectra were recorded on a Cary 219 spectrophotometer. Electron paramagnetic resonance spectra were obtained by using a Varian E-109 spectrometer with DPPH used as the *g* value standard. Cyclic voltammograms were obtained with a PAR Model 174A potentiostat at scan rates ranging from 50 to 1000 mV/s. A platinum-wire working electrode and a platinum-coil auxiliary electrode were used. TBAP was used as the supporting electrolyte, a Ag/AgCl reference electrode was used, and the ferrocene/ferrocenium couple was used as an internal standard. $E_{1/2}$ for oxidation for 10^{-3} M ferrocene vs. Ag/AgCl is 0.52 V.

Crystallographic Structure Determination on $[Na(CH_3OH)_4][V(O_2C_6H_2(t\text{-}Bu)_2)_3]$. The crystal used for this investigation was obtained from a reaction of V^{2+} with 3,5-di-*tert*-butylcatechol in a CH_3OH solution containing $NaOCH_3$. Crystals formed as large parallelepipeds directly from solution. These crystals were determined to be identical with crystals obtained by using the synthetic procedure above. Even though a relatively large crystal was used for data collection, it was observed to diffract very poorly. This is often related to molecular disorder, and such was found to be the case in this structure determination. Carbon atoms of catecholate *tert*-butyl groups refined with elongated anisotropic thermal parameters due to apparent rotational disorder. Methanol solvate molecules associated with the sodium ion suffered from severe positional disorder. Two of the solvate molecules are coordinated to the cation to give a slightly distorted octahedron of oxygen atoms about the Na^+ ion. The remaining two methanol molecules are hydrogen-bonded to those coordinated to the sodium. The locations of the V atom and other atoms of the inner coordination sphere were determined by direct methods. Details of procedures used for data collection and structure determination are given in Table IV. Final positional and isotropic thermal parameters for all atoms are listed in Table V. Tables containing anisotropic thermal parameters and structure factors are available as supplementary material.

Acknowledgment. This research was supported by the National Institutes of Health through Grant GM23386 (C.G.P.) and the National Science Foundation through Grants RIT-8409039 (N.R.G., C.G.P.) and CHE-8503222 (C.G.P.). MEC was the recipient of a University of Colorado Graduate Fellowship. We wish to thank Prof. Carl Koval for assistance with electrochemistry experiments.

Registry No. $V(O_2C_6Cl_4)_3\cdot 4C_6H_6$, 103935-66-6; $[Na(CH_3OH)_4][V(O_2C_6Cl_4)_3]$, 103935-64-4; $V(CO)_6$, 14024-00-1; $[Na(diglyme)_2][V(CO)_6]$, 15531-13-2; $[Na(CH_3OH)_4][V(O_2C_6H_2(t\text{-}Bu)_2)_3]$, 104011-74-7; tetrachloro-1,2-benzoquinone, 2435-53-2; 3,5-di-*tert*-butyl-1,2-benzoquinone, 3383-21-9.

Supplementary Material Available: A table containing anisotropic thermal parameters (2 pages) for the $Na[V(DBCat)_3]\cdot 4CH_3OH$ structure determination; a table of calculated and observed structure factors (12 pages). Ordering information is given on any current masthead page.

---

(22) Werner, R. P. M.; Podall, H. E. *Chem. Ind.* (*London*) **1961**, 144.

(23) This general synthetic procedure has also been used to prepare related complexes of 1,2-naphthoquinone and 9,10-phenanthrenequinone.

Contribution from the Laboratoire de Chimie des Polymères Inorganiques, Université Pierre et Marie Curie, 75252 Paris Cedex 05, France, and Laboratoire de Cinétique Chimique, Université Pierre et Marie Curie, 75005 Paris, France

Derivatives of Tetrathiotungstate(VI). Synthesis and Structure of $[W_2(S)_2(SH)(\mu\text{-}\eta^3\text{-}S_2)(\eta^2\text{-}S_2)_3]^-$

F. Sécheresse,*[†] J. M. Manoli,[‡] and C. Potvin[‡]

Received May 31, 1985

Acidification (HCl in CH_3CN) of a solution of $[PPh_4]_2WS_4$ in CH_3CN leads to the formation of the dinuclear anion $[W_2S_{11}H]^-$. The complex crystallizes in the space group $C2/c$ ($Z = 4$) with unit cell dimensions $a = 13.126$ (1) Å, $b = 23.272$ (2) Å, $c = 11.499$ (6) Å, and $\beta = 96.83$ (4)°; final $R = 0.0505$ based on 5225 reflections collected and 1849 used. Each tungsten is ligated by six sulfur atoms in approximatively pentagonal-pyramidal coordination geometry. The two pyramids share a corner with a W–S(3)–W bridge angle of 90.0 (2)°. The axial position of each pyramid is occupied by a terminal sulfido group, and the equatorial positions are occupied by a bridging and simultaneous side-on disulfido (S_2^{2-}) group, a terminal disulfido group, and an SH^- ligand. ^1H NMR spectra reveal indirectly the thiol proton. Electronic spectral assignments are proposed.

Interest in sulfur-containing compounds of Mo and W has grown with respect to their implications in bioinorganic chemistry[1] and catalysis.[2] "Soluble metal sulfides"[3] $M_nS_m^{2-}$ (M = Mo, W) constitute a new class of transition-element compounds. The chemistry of binary soluble Mo–S anions is by far the most highly developed, showing a wide range of stoichiometries: MoS_9^{2-},[4] $Mo_2S_8^{2-}$,[5] $Mo_2S_{10}^{2-}$,[6] $Mo_2S_{12}^{2-}$,[7] $Mo_3S_9^{2-}$,[8] and $Mo_3S_{13}^{2-}$.[9] With

---

[†] Laboratoire de Chimie des Polymères Inorganiques.

[‡] Laboratoire de Cinétique Chimique.

(1) Stiefel, E. I. *Prog. Inorg. Chem.* **1977**, *22*, 1.

(2) Massoth, F. E. *Adv. Catal.* **1978**, *87*, 265.

(3) Sola, J.; Do, Y.; Berg, J. M.; Holm, R. H. *J. Am. Chem. Soc.* **1983**, *105*, 7794.

(4) Simhon, E. D.; Baezinger, N. C.; Kanatzidis, M.; Draganjac, M.; Coucouvanis, D. *J. Am. Chem. Soc.* **1981**, *103*, 1218–1219.

0020-1669/86/1325-3967$01.50/0

Table I. Crystal Data for $(PPh_4)W_2S_{11}H$

formula	$C_{24}H_{21}PW_2S_{11}$
mol wt	1060
a, Å	13.121 (6)[a]
b, Å	23.272 (2)
c, Å	11.499 (6)
β, deg	96.83 (4)
V, Å^3	3486.42
space group	$C2/c$
Z	4
cryst dimens, mm	0.084 × 0.057 × 0.348
μ(Mo Kα), cm^{-1}	73.7
transmission factors	0.71–0.82
scan mode	θ–2θ
scan range (2θ) deg	4–60
scan rate, deg min^{-1}	0.42
scan width, deg	0.8
stds (measd every 1 h)	$0\bar{6}0$, 733, $06\bar{6}$
no. of reflcns measd[c]	5225
no. of data used ($F_o^2 > 3\sigma(F_o^2)$)	1849
no. of var refined	181
R[b]	0.0505
R_w	0.0575

[a] From a least-squares refinement of the setting angles of 20 reflections. [b] The function minimized was $\sum w(|F_o| - |F_c|)^2$ where $w = 4F_o^2/\sigma^2(F_o^2)$. The unweighted and weighted residuals are defined as $R = (\sum||F_o| - |F_c||)/\sum|F_o|$ and $R_w = |\sum w(|F_o| - |F_c|)^2/\sum w|F_o|^2|^{1/2}$. [c] T = 25 °C.

tungsten a less extensive set of structurally defined thiometalates has been already reported: $W_3S_8^{2-}$,[10] $W_3S_9^{2-}$,[11] and $W_4S_{12}^{2-}$.[12] Acidification of WS_4^{2-} in nonaqueous solvents produces doubly bridged polynuclear complexes[13] where the metallic centers are partially reduced. The formation of $W_3S_9^{2-}$ and $W_4S_{12}^{2-}$ probably involves an internal redox reaction between coordinated reducing S^{2-} ions and W centers.[8] For such redox schemes, intermediates containing both/either reduced tungsten and/or oxidized sulfur were expected but not isolated. These observations prompted the exploration of soluble W–sulfides of different nuclearity. We have isolated in the course of this work a new dinuclear soluble tungsten sulfide, $[W_2(S)_2(SH)(S_2)_4]^-$, involving different sulfur ligation modes that are described in this paper.

Experimental Section

Preparation of $(PPh_4)W_2S_{11}H$. All manipulations were carried out in air. Chemicals were used as purchased.

Method A. The title compound was prepared by dissolving 0.5 g of $(PPh_4)_2WS_4$ (0.5 mmol) in 45 mL of CH_3CN to which 5 mL of 0.5 N HCl (in MeCN) had been added with stirring. The mixture was stirred for 1 h at room temperature and then cooled to 0 °C. The red crystals that deposited after 24 h were filtered off, washed with 20 mL of absolute ethanol, and dried under vacuum (yield 10%). Anal. Calcd for $C_{24}H_{21}PW_2S_{11}$: C, 27.16; P, 3.02; S, 32.20; W, 34.7. Found: C, 26.77; P, 2.88; S, 32.59; W, 32.48.

The filtrate was allowed to stand at 0 °C for an additional 24 h. Besides crystals of $(PPh_4)W_2S_{11}H$ an insoluble brown byproduct deposited.

Table II. Positional Parameters and Standard Deviations for the Atoms of $(PPh_4)W_2S_{11}H$[a]

atom	x	y	z
W	0.13441 (5)	−0.09599 (4)	−0.22820 (7)
S(6)	0.2412 (4)	−0.1326 (3)	−0.3650 (5)
S(1)	0.0220 (4)	−0.1357 (2)	−0.1022 (4)
S(2)	0.1223 (4)	−0.1921 (2)	−0.1646 (4)
S(5)	0.2428 (4)	−0.0553 (3)	−0.1068 (6)
S(3)	0.0000	−0.0208 (3)	−0.2500
P	0.5000	−0.2722 (3)	−0.2500
S(41)	0.1615 (9)	−0.0496 (6)	−0.403 (1)
S(42)	0.0907 (8)	−0.0289 (5)	−0.391 (1)
C(11)	0.327 (1)	0.3059 (9)	0.348 (2)
C(12)	0.393 (1)	0.3180 (9)	0.263 (1)
C(13)	0.379 (1)	0.3652 (9)	0.197 (2)
C(14)	0.298 (2)	0.402 (1)	0.215 (2)
C(15)	0.236 (2)	0.390 (1)	0.300 (2)
C(16)	0.248 (2)	0.340 (1)	0.367 (2)
C(21)	0.532 (1)	0.177 (1)	0.116 (2)
C(22)	0.474 (1)	0.2296 (8)	0.122 (1)
C(23)	0.400 (2)	0.2458 (9)	0.034 (1)
C(24)	0.386 (2)	0.211 (1)	−0.065 (2)
C(25)	0.447 (2)	0.161 (1)	−0.076 (2)
C(26)	0.520 (1)	0.143 (9)	0.014 (2)

[a] S(41) and S(42) sulfur atoms in positional disorder with occupancy factor of 0.5.

Method B. $(PPh_4)_2WS_4$ (0.5 g, 0.5 mmol) was dissolved in 45 mL of CH_3CN, and solid elemental sulfur (0.032 g, 1 mmol) was added. The mixture was refluxed in air with stirring for ca. $^1/_4$ h. The resulting red-brown solution was cooled to ambient temperature, filtered, and acidified with a solution of HCl (2.5 mmol) in 5 mL of MeCN. After 10 min of stirring the mixture was allowed to stand at room temperature. Within 30 min, red-brown crystals were isolated and washed as previously described. Additional crystals were obtained from the filtrate by fractionated crystallization (yield 40%). No brown byproduct was formed via this route. The electronic and IR spectra of the crystals were identical with those obtained with method A.

Physical Measurements. Electronic spectra were recorded at 20 °C on a KONTRON 810 spectrophotometer between 600 and 200 nm. Solutions of the compound in DMF were about 1 mg mL^{-1}: shoulder at 475 nm (ϵ = 1.34 10^3 M^{-1} cm^{-1}).

Infrared spectra (KBr pellet) were recorded on a Perkin-Elmer 580 B spectrophotometer: 508 (shoulder in the cation band), 340 (w), 325 (w), 309 (w) cm^{-1}.

^{1}H NMR spectra were obtained at 298 K with a Bruker WM 500 spectrometer in the Groupe de Mesures Physiques de Paris Centre. The compound was dissolved in $(CD_3)_2SO$.

Crystal Structure Determination. Intensity data were collected on a Philips PW 1100 four-circle diffractometer using graphite-monochromatized Mo Kα radiation and a θ–2θ flying-step scan technique. Specific parameters pertaining to the data collection are reported in Table I. The intensities were corrected for polarization and Lorentz effects. Absorption corrections were performed. The centrosymmetric space group $C2/c$ was assumed and gave satisfactory refinements. The structure was solved by the heavy-atom method. A three-dimensional Patterson map revealed the position of the tungsten atom.[14] The phosphorus atom and five sulfur atoms were located in subsequent Fourier syntheses following least-squares refinements of the input atomic coordinates. The refinement with isotropic thermal parameters of all located atoms gave a R value of 0.17. At this stage a difference Fourier synthesis revealed two similar peaks of equal electron density separated by 1 Å and 12 other peaks attributed to the carbon atoms of the phenyl rings. The relative weights of these peaks (half a sulfur atom) suggested that a new sulfur atom was in half-occupancy at two different positions. Refinement of this model led to an occupancy factor of 0.51 (1). This result verifies the assumed 50/50 positional disorder.

Additional cycles of refinement with anisotropic temperature factors for all atoms and fixed occupancy factor for disordered atoms converged to R = 0.0505 and R_w = 0.0575, respectively. In addition, the phenyl

---

(5) Pan, W. H.; Harmer, M. A.; Halbert, T. R.; Stiefel, E. I. *J. Am. Chem. Soc.* **1984**, *106*, 459–460.

(6) Draganjac, M.; Simhon, E.; Chan, L. T.; Kanatzidis, M.; Baezinger, N. C.; Coucouvanis, D. *Inorg. Chem.* **1982**, *21*, 3321–3332.

(7) Müller, A.; Nolt, W. O.; Krebs, B. *Angew. Chem., Int. Ed. Engl.* **1978**, *17*, 279.

(8) Pan, W. H.; Leonowicz, M. E.; Stiefel, E. I. *Inorg. Chem.* **1983**, *22*, 672–678.

(9) Müller, A.; Sarkar, S.; Bhattacharyya, R. G.; Pohl, S.; Dartmann, M. *Angew. Chem., Int. Ed. Engl.* **1978**, *17*, 535.

(10) Bhaduri, S.; Ibers, J. A. *Inorg. Chem.* **1986**, *25*, 3.

(11) (a) Königer-Ahlborn, E.; Müller, A. *Angew. Chem.* **1975**, *87*, 598; *Angew. Chem., Int. Ed. Engl.* **1975**, *14*, 573. (b) Müller, A.; Bögge, H.; Krickemeyer, E.; Henkel, G.; Krebs, B. *Z. Naturforsch, B: Anorg. Chem., Org. Chem.* **1982**, *37B*, 1014–1019.

(12) Sêcheresse, F.; Lefebvre, J.; Daran, J. C.; Jeannin, Y. *Inorg. Chem.* **1982**, *21*, 1311–1314.

(13) (a) Müller, A.; Diemann, E.; Jostes, R.; Bögge, H. *Angew. Chem., Int. Ed. Engl.* **1981**, *20*, 934. (b) Sêcheresse, F.; Lavigne, G.; Jeannin, Y.; Lefebvre, J. *J. Coord. Chem.* **1981**, *11*, 11.

(14) All calculations have been preformed by using the CII IRIS 80 computer of the Atelier d'Informatique. In addition to various local programs, modified versions of the following were employed: Zalkin's FORDAP Fourier summation progran; Johnson's ORTEP thermal ellipsoid plotting program; Busing and Levy's ORFFE error function program; Ibers' NUCLS full-matrix program, which in its nongroup form closely resembles Busing and Levy's ORFLS program.

Table III. Bond Lengths (Å)[a] and Angles (deg)[a] for $(PPh_4)W_2S_{11}H$

	Tungsten Surrounding		
W---W	3.503 (1)		
W-S(1)	2.374 (5)		
W-S(2)	2.366 (5)		
W-S(3)	2.476 (5)		
W-S(5)	2.096 (6)	S(1)-S(2)	2.049 (7)
W-S(6)	2.384 (5)	S(6)-S(41)	2.21 (1)
W-S(41)	2.35 (1)	S(3)-S(42)	2.13 (1)
W-S(42)	2.46 (1)	S(41)-S(42)	1.07 (1)
S(1)-W-S(2)	51.2 (2)		
S(2)-W-S(6)	86.1 (2)		
S(6)-W-S(5)	101.3 (2)		
S(5)-W-S(3)	99.6 (2)		
S(3)-W-S(1)	81.4 (1)		
S(41)-W-S(1)	150.5 (3)	S(42)-W-S(1)	127.4 (3)
S(41)-W-S(2)	136.2 (3)	S(42)-W-S(2)	145.2 (3)
S(41)-W-S(3)	76.6 (3)	S(42)-W-S(3)	51.2 (3)
S(41)-W-S(5)	101.8 (3)	S(42)-W-S(5)	107.3 (3)
S(41)-W-S(6)	55.8 (3)	S(42)-W-S(6)	80.1 (3)
	Sulfur Surrounding		
W-S(1)-S(2)	64.2 (2)		
W-S(2)-S(1)	64.6 (2)	W-S(3)-W	90.0 (2)
W-S(3)-S(42)	63.9 (3)	W-S(6)-S(42)	51.0 (2)
W-S(42)-S(3)	64.9 (3)	W-S(42)-S(6)	49.0 (2)

[a] Estimated standard deviations in parentheses refer to the last significant digits.

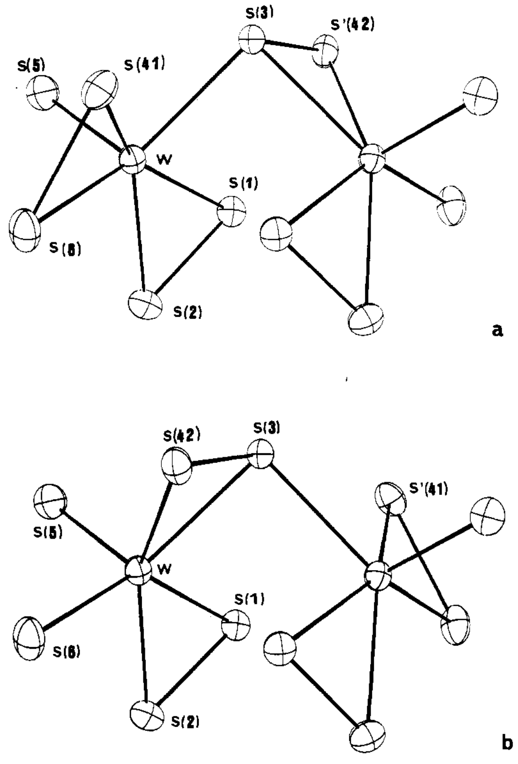

Figure 1. Perspective views (50% ellipsoids) of the two derived configurations of $W_2S_{11}H^-$ with S(41) and S'(42) representing the half-occupancy sites of the S(4) sulfur atom.

hydrogen atoms were included in the structure factor calculations at their calculated positions (C–H = 0.95 Å, B = 6 Å^2) but not refined.

Values of the atomic scattering factors for all atoms were obtained from the usual source.[15] Final positional parameters are listed in Table II. Bond distances and angles for the $W_2S_{11}H^-$ anion are given in Table III. The distances in the PPh_4^+ cation, anisotropic thermal parameters for all atoms, calculated hydrogen positions, mean planes, and observed and calculated structure factors are available as supplementary material.

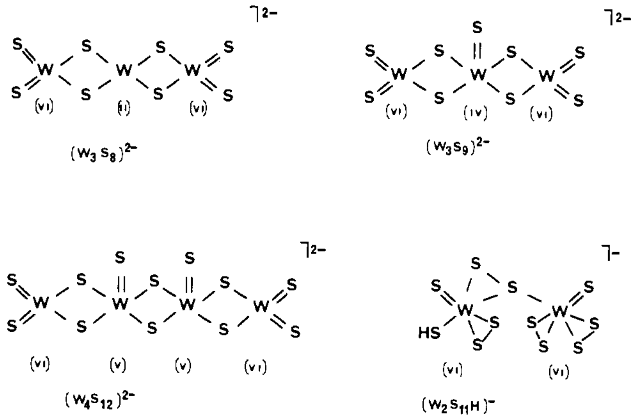

Figure 2. Structure types of tungsten–sulfido anions.

Results and Discussion

Crystal Structure. Refinements following electron density maps suggested the superposition of the two dinuclear structures shown in perspective in Figure 1. The first configuration (a) is obtained by locating the disordered sulfur atom S(4) in the S(41) and S'(42) sites while the second (b) is obtained by locating the S(4) atom in the S(42) and S'(41) sites. The superposition of these two unsymmetrical geometries is consistent with the evidence of a twofold axis passing through S(4) and also with occupancy factors of 0.50 for S(4). Each tungsten atom is surrounded by six sulfur atoms in a distorted pyramidal arrangement. The axial position of each pyramid is occupied by the terminal sulfido group S(5). The W atoms are each 0.50 and 0.55 Å above the mean-squares plane of the five basal sulfur atoms. The two distorted pyramidal units are connected via a corner (S(3) sulfur atom).

The anion adopts the syn geometry. The dihedral angle between the base planes of the two moieties has a very low and unexpected value of 51° while the W–S(3)–W bridge angle is 90.0 (2)°.

Structure types of tungsten–sulfido anions that have been crystallographically established are schematically illustrated by Figure 2, including a configuration of $[W_2S_{11}H]^-$.

The most noteworthy structural feature is the evidence of two types of persulfido ligands in the anion. The two tungsten atoms are linked via a $(\mu\text{-}\eta^3\text{-}S_2)$ ligand (S(3), S(42)), which displays a simultaneous end-on coordination (to one W atom) as well as a side - on coordination (to the other W atom). This bonding scheme, which refers to types I-b in the classification of Müller and co-workers, has not been so far observed in solid-state structures. This less frequent S_2^{2-} bridging mode occurs in complexes such as $[Mo_4(NO)_4S_{13}]^{4-}$,[17] $[W_2S_8OH_3]^-$,[18] $[(MeC_5H_4)_2Fe_2S_4(CO)]$[19] $[(Me_5C_5)_2Mo_2S_{10}]$,[20] and $[Mo_2Fe_6S_8(S_2)_2(SC_6H_4Br)_6]^{4-}$.[21]

In addition, one or two $(\eta^2\text{-}S_2)$ groups, according to the two different configurations, are end-on coordinated to each W atom. These two types of coordination have been previously encountered for Mo complexes only.[20,22] The S(1)–S(2) distances in the disulfide ligands are in good agreement with the data usually

---

(15) Cromer, D. T.; Waber, J. T. *International Tables for X-Ray Crystallography*; Kynoch: Birmingham, England, 1974; Vol. IV, Tables 2.2 A, 2.3.1.

(16) (a) Müller, A.; Jaegermann, W.; Enemark, J. H. *Coord. Chem. Rev.* **1982**, *46*, 246 and references therein. (b) Müller, A.; Jaegermann, W. *Inorg. Chem.* **1979**, *18*, 2633.

(17) Müller, A.; Eltzner, W.; Mohan, N. *Angew. Chem., Int. Ed. Engl.* **1979**, *18*, 168.

(18) Sécheresse, F.; Lefebvre, J.; Daran, J. C.; Jeannin, Y. *Inorg. Chim. Acta* **1981**, *54*, L175–L176.

(19) Giannoti, C.; Ducourant, A. M.; Chenaud, H.; Chiaroni, A.; Riche, C. *J. Organomet. Chem.* **1977**, *140*, 289.

(20) Rakowski-Dubois, M.; Dubois, D. L.; Van Derveer, M. C.; Haltiwanger, R. C. *Inorg. Chem.* **1981**, *20*, 3064.

(21) Kovacs, J. A.; Bashkin, J. K.; Holm, R. H. *J. Am. Chem. Soc.* **1985**, *107*, 1784.

(22) Müller, A.; Ritner, W.; Mohan, N. *Angew. Chem., Int. Ed. Engl.* **1975**, *18*, 168.

(23) Sécheresse, F.; Lefebvre, J., manuscript in preparation.

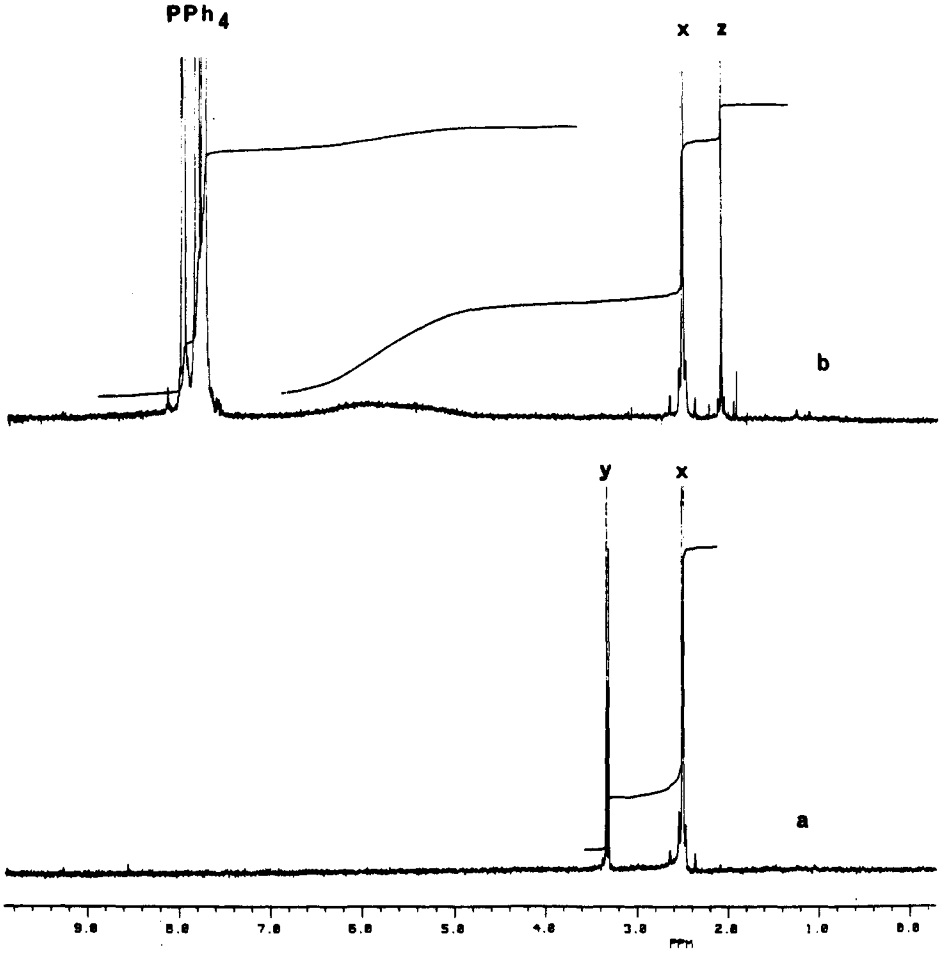

Figure 3. ^1H NMR spectra of $(PPh_4)W_2S_{11}H$ in $(CD_3)_2SO$ at 25 °C: (a) spectrum of deuterated $(CD_3)_2SO$, the features marked being due to residual solvent protons (x) and water (y); (b) spectrum of the compound dissolved in $(CD_3)_2SO$, the features marked x and z being respectively the residual solvent protons and CH_3CN solvent used in the syntheses.

reported for disulfido groups,[16] while the S(41)–S(6) and S-(42)–S(3) distances of 2.21 (1) and 2.13 (1) Å, among the largest S–S reported, are certainly complicated by the disorder involving S(41) and S′(42). The terminal W–S(5) bond distance of 2.096 (6) Å is characteristic of a double W=S bond as in $W_3S_9^{2-}$ (2.070 (1) Å)[11] or in $W_4S_{12}^{2-}$ (2.069 (2) Å).[12]

The other terminal W–S bonds, W–S′(6) in configuration a or W–S(6) in configuration b, are larger (2.384 (5) Å) than expected for W=S terminal bond distances.

This supports the proposal that this lengthening is attributed to a hydrogenosulfido hydrogen atom yielding an SH^- ligand. The hydrogen of the SH group could not be located in Fourier difference maps owing to its half-occupancy factor. No band due to SH vibration is observed in IR spectra.

Additional support for this hypothesis is provided by the study of the ^1H NMR spectra of the complex. The metal–metal distance of 3.503 (1) Å clearly precludes any direct interaction between the two tungsten atoms.

^1H NMR Spectroscopy. Proton NMR spectra of the compound in $(CD_3)_2SO$ solution at 25 °C are shown in Figure 3. Attempts to locate the proton resonance in the region expected for a thiol proton were unsuccessful. The peak of water protons in Figure 3a disappears when the complex is dissolved in $(CD_3)_2SO$. The most significant feature of the spectrum in Figure 3b is the appearance of a broad resonance at ca. 5.6 ppm. This broadening is indicative of a fast-exchange regime. The signal is probably be due to an exchange between the thiol proton and the water protons of $(CD_3)_2SO$. Consistent with this proposal is the absorption of the intensities ratios. In Figure 3b we find the intensity ratio ortho H:meta H:para H:exchange protons of ~4:8:8:1.6. Signal intensities between the water protons and the residual solvent protons of $(CD_3)_2SO$ in the spectrum in Figure 3b correspond to the ratio 1.6:2.9. Furthermore, the same ratio observed in Figure 2a leads to a 0.63:2.9 value. These calculations provide reasonable evidence that the complex possesses an exchange proton by 1 mol.

Electronic Spectra. In the three-centered core

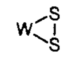

the antibonding orbital π* of the S_2^{2-} group splits into two components:[16,24] a π*h orbital located in the WS_2 plane and strongly interacting with the metal and a π*v orbital perpendicular to the WS_2 plane and weakly interacting with the metal.

The absorption observed at 475 nm on the electronic spectrum of $W_2S_{11}H^-$ should correspond to the π*v→d(metal) transition. This CT is confirmed for peroxo complexes by the dependence of the position of the band upon oxidation state of the metal. Spectra of

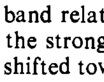

complexes with end-on coordinated disulfido groups exhibit a band of low energy about 500 nm[16] corresponding also to the π*v → d(metal) CT. A second band related to the π*h→d transition is expected. Because of the strong stabilization of the orbital bonding this transition is shifted toward higher energies. In the spectra of $W_2S_{11}H^-$ this second band is not observed, owing to the high oxidation state of the W atoms.[25] In less oxidized complexes $Mo_3S(S_2)_6^{2-}$, $Mo_3S(S_2)_3Cl_4$, $Mo_2(S_2)Cl_6$, and

---

(24) Lever, A. B. P.; Gray, H. B. *Inorg. Chem.* **1977**, *11*, 348.
(25) Truck, D. G.; Walters, R. H. *Inorg. Chem.* **1963**, *2*, 428.

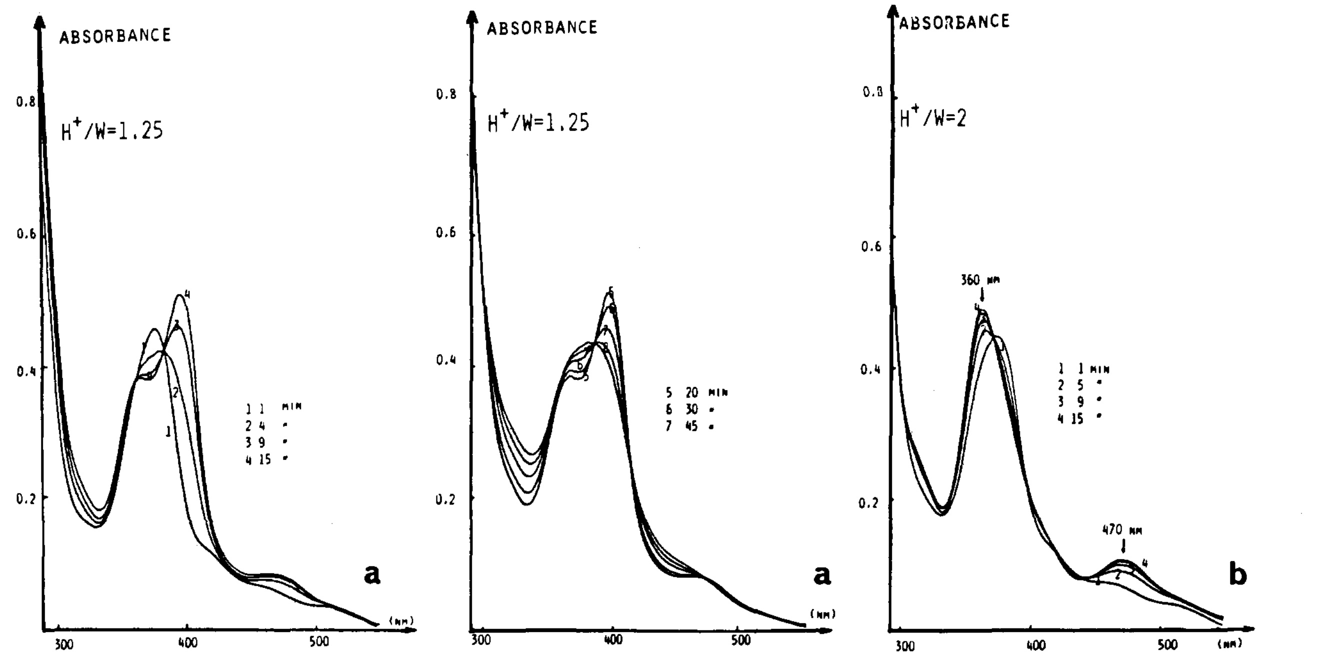

Figure 4. UV–vis spectra for WS_4^{2-} in acidified acetonitrile solutions: (a) [W] = 10^{-3} mol L^{-1}, x = 1.25, cell 1 mm; (b) [W] = 10^{-3} mol L^{-1}, x = 2, cell 1 mm.

$Mo_2O_2S_2(S_2)_2^{2-}$, the second band is observed at about 365 nm.[16]

Synthesis. The reaction of $(PPh_4)_2WS_4$ with HCl in MeCN either under a dinitrogen atmosphere or in the air produces the three soluble metal sulfides $W_3S_9^{2-}$, $W_4S_{12}^{2-}$, and $W_2S_{11}H^-$ related to the value of $x = HCl/WS_4^{2-}$.

(i) $0 < x < 1$. The first electronic spectrum recorded 1 min after addition of HCl showed absorption at 395 nm, corresponding to the evidence of unreacted WS_4^{2-}.

(ii) $1 < x < 1.5$. Figure 4a shows a set of spectra corresponding to x = 1.25. Only one maximum is observed at 370 nm on the electronic spectrum recorded just after addition of HCl, showing that WS_4^{2-} fully reacted at once. In this acidic range, the peak observed at 370 nm is not dependent upon x values and appears proportional to the concentration of tungsten, so characterizing a new compound, namely A ($\epsilon_{370} = 4.40 \times 10^3$ M^{-1} cm^{-1}). Within 30 min the band at 370 nm splits into two components characteristic of another new intermediate, B. The final spectra are analyzed in terms of a mixture of $W_3S_9^{2-}$ and $W_4S_{12}^{2-}$.

(iii) $x > 1.5$. Figure 4b represents a set of spectra obtained for x = 2. The first spectrum recorded within 1 min is strictly the same as that above ($\epsilon_{370} = 4.4 \times 10^3$ M^{-1} cm^{-1}). After 30 min this band is replaced by the two maximums already observed at 360 and 470 nm. Furthermore, the set of spectra is passing through two isosbestic points at 370 and 450 nm, respectively, showing a simple conversion of A into only one absorbing species. A limit is reached (30 min), and absorbance remains unchanged. The intensities of the peaks at 360 and 470 nm are independent of x and are characteristic of a new compound, B ($\epsilon_{360} = 4.9 \times 10^3$ M^{-1} cm^{-1}, $\epsilon_{470} = 10^3$ M^{-1} cm^{-1}). Within a few hours the spectrum slowly changes, showing a mixture of $W_3S_9^{2-}$ and $W_4S_{12}^{2-}$ for $x < 3$ or the formation of $W_2S_{11}H^-$ for $x > 3$.

The formation of $W_3S_9^{2-}$, $W_4S_{12}^{2-}$, and $W_2S_{11}H^-$ from WS_4^{2-} clearly proceeds through two intermediates, A and B,[23] according to the scheme

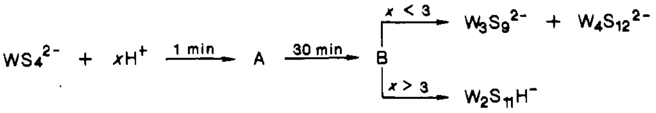

The route of preparation of $W_2S_{11}H^-$ is directly deduced (x = 5) from the spectroscopic observations.

The low yield (10–40%) of the preparation is related to the different sulfur coordination modes borne by tungsten. The disulfide ligands (S_2^{2-}) in $W_2S_{11}H^-$ are prepared in situ by oxidation of S^{2-} groups of WS_4^{2-} under acidification without external addition of S_2^{2-} dianions.

Registry No. $(PPh_4)W_2S_{11}H$, 103834-84-0; $(PPh_4)_2WS_4$, 14348-11-9; sulfur, 7704-34-9.

Supplementary Material Available: Listings of cation bond lengths and angles, mean planes, anisotropic thermal parameters for non-hydrogen atoms, and calculated positional parameters for H atoms (4 pages); a listing of structure factor amplitudes (12 pages). Ordering information is given on any current masthead page.